Applied Mathematics Letters 93 (2019) 98–104

Contents lists available at ScienceDirect

Applied Mathematics Letters

www.elsevier.com/locate/aml

Multiscale models of blood flow in the compliant aortic bifurcation☆

Tatyana Dobroserdova [a], Fuyou Liang [b,c], Grigory Panasenko [d], Yuri Vassilevski [e,*]

[a] *Marchuk Institute of Numerical Mathematics, Russian Academy of Sciences, Russian Federation*
[b] *Shanghai Jiao Tong University, China*
[c] *Sechenov University, Russian Federation*
[d] *Insitut Camille Jordan UMR CNRS 5208, France*
[e] *Marchuk Institute of Numerical Mathematics, Russian Academy of Sciences, Moscow Institute of Physics and Technology, Sechenov University, Moscow, Russian Federation*

ARTICLE INFO

Article history:
Received 22 November 2018
Received in revised form 25 January 2019
Accepted 25 January 2019
Available online 4 February 2019

Keywords:
Multiscale modeling
3D fluid–structure interaction
Aortic bifurcation

ABSTRACT

The paper introduces and compares several multiscale models of blood flow in the aortic bifurcation against a reference 3D FSI solution [1]. All these models reproduce the 3D flow in a small neighborhood of the junction. A three-scale model composed of 3D, 1D and 0D equations provides flow rate and pressure close to the reference 3D FSI solution.

1. Introduction

Our research was motivated by the comparative study of 3D fluid–structure interaction (FSI) and 1D hemodynamic simulations for different parts of human arterial tree [1]. The study demonstrates good agreement in averaged (at vessel cross-sections) blood pressures and flow rates of both models. Therefore, one can use low-cost 1D hemodynamic simulations in clinical applications which need the averaged flow rates and pressures. However, if clinicians want to visualize or postprocess 3D blood flow in a small part of the arterial tree and cannot afford to wait for the result of time-consuming 3D FSI modeling, they have to use a multiscale approach. In this approach, only a region of particular interest has 3D flow model, the other part of the arterial tree is represented by a combination of 1D network and 0D models. However, even in

☆ The work of G. Panasenko has been supported by grant 09.3.3-LMT-K-712 of the European Social Fund. The work of the other co-authors has been supported by the RFBR (Russia) grants 17-01-00886, 17-51-53160, 18-31-20048.

* Corresponding author.
E-mail addresses: dobroserdovatk@gmail.com (T. Dobroserdova), fuyouliang@sjtu.edu.cn (F. Liang), grigory.panasenko@univ-st-etienne.fr (G. Panasenko), vasilevs@dodo.inm.ras.ru (Y. Vassilevski).

https://doi.org/10.1016/j.aml.2019.01.037
0893-9659/

the reduced 3D domain, the 3D FSI simulation is still computationally expensive, and the practical question arises: can a 3D flow model with rigid walls be relevant for visualization and postprocessing? The answer depends on the part of the arterial tree we are interested in.

It is known [2] that the 3D flow induced by a contracting pump in a compliant vessel differs essentially from that in a vessel with rigid walls. In the rigid vessel, the pressure waveform everywhere is similar and synchronous with that at the inlet, only amplitude being scaled according to localization of such measurement. The volume flow rate does not change at any cross-section of the vessel. Therefore, in general, one cannot expect similar waveforms in vessels with compliant and rigid walls. However, the aortic bifurcation is known to be the major site of pressure wave reflection [2]. Physically, this implies that the bifurcation behaves as an inserted patch with stiffer walls and considering the bifurcation as a rigid vessel may give an acceptable result.

The paper introduces and compares several multiscale models of blood flow in the aortic bifurcation against the reference solution of a 3D fluid–structure interaction problem computed in [1]. In contrast to fast 1D hemodynamic solvers, all these models reproduce the 3D flow in a small neighborhood of the junction and therefore are more efficient than the reference 3D FSI solver. A three-scale model incorporating 3D Navier–Stokes equations in the junction vicinity, 0D models of a compliant sphere at the inlet and outlet of the 3D model, and 1D models at the inlet and outlet segments of the bifurcation provides flow rate and pressure close to the reference 3D FSI solutions.

The paper is organized as follows. Section 2 describes an idealized aortic bifurcation with physiologically relevant sizes and parameters of blood flow and the aortic wall. Section 3 introduces the reference 3D fluid–structure interaction model and the 1D hemodynamic model. Section 4 describes reduced multiscale models with various degrees and meanings of reduction. Section 5 presents comparative results of numerical simulation by these models and a discussion of these results.

2. Experimental setting

We address an idealized model of the aortic bifurcation [1,3] with an inlet segment (abdominal aorta, marked with subscript a) and two equal branch segments (iliac arteries marked with subscript i) forming the angle 47.9 degrees. They are represented by three cylinders Ω_a, $\Omega_{i,1}$, $\Omega_{i,2}$ with lengths $L_a = 8.6$ cm, $L_i = 8.5$ cm, radii $r_a = 0.86$ cm, $r_i = 0.60$ cm, diastolic cross-sectional areas $A_a = 1.8062$ cm^2, $A_i = 0.9479$ cm^2, wall thicknesses $h_a = 1.032$ mm, $h_i = 0.72$ mm, Young's modulii $E_a = 500$ kPa, $E_i = 700$ kPa, density $\rho_w = 1$ g/cm^3. The blood is assumed to have viscosity $\mu_b = 4$ mPa s and density $\rho_b = 1060$ kg/m^3 and mean flow rate $\bar{Q}_a = 0.4791$ l/min.

The blood velocity profile at the inlet is assumed to be axisymmetric and constant in shape, the axial velocity being equal to

$$u(\xi, t) = U(t)n^{-1}(n+2)[1 - (\xi r^{-1})^n], \tag{2.1}$$

where r is the lumen radius, ξ is the radial coordinate, $n = 9$ is the polynomial order providing a good approximation of experimentally measured profile, $U(t)$ is the axial blood flow velocity averaged over the cross-section. The flow rate $Q(t)$ (the integral of $u(\xi, t)$ over the inlet) is a given function of time [3], and $U(t)$ can be recovered from $Q(t)$ if cross-sectional area is known. Depending on the model, one may impose the velocity (for rigid wall models) or the flow rate (for compliant wall models) as the boundary condition on the inlet. Each terminal vessel is coupled with a three-element 0D Windkessel model:

$$Q(1 + R_1/R_2) + CR_1\partial Q/\partial t = (P - P_{out})/R_2 + C\partial P/\partial t, \tag{2.2}$$

where Q and P are unknown flow rate and pressure; $R_1 = 6.8123 \cdot 10^7$ Pa s m^{-3} and $R_2 = 3.1013 \cdot 10^9$ Pa s m^{-3} are resistances; $C = 3.6664 \cdot 10^{10}$ m^3 Pa^{-1} is compliance; $P_{out} = 0$ is the pressure at which flow to the microcirculation ceases [1]. Windkessel models represent downstream vasculature.

The values of interest are the flow rate and the pressure as functions of time at the cross-section located at the beginning of branching (the intersection of vessels centerlines called the junction).

3. Conventional models of blood flow in compliant aortic bifurcation

3.1. Full 3D FSI model

Let a time-dependent domain (blood vessel) $\Omega \subset \mathbb{R}^3$ be partitioned into subdomains Ω_b and Ω_w occupied by blood and vessel wall, respectively, with the interface $\Gamma_{bw} \coloneqq \partial\Omega_b \cap \partial\Omega_w$. The blood and the vessel wall are assumed to be incompressible media, with the densities ρ_b and ρ_w and the Cauchy stress tensors $\boldsymbol{\sigma}_b$, $\boldsymbol{\sigma}_w$. The velocity field $\mathbf{v}$ is assumed to be continuous at Γ_{bw}, the pressure p may jump across Γ_{bw}. If one assumes that the vessel wall kinematics is linearized, the conservation of momentum equations for the wall and blood written in the Eulerian coordinates, respectively, takes the form [1]

$$\frac{\partial \mathbf{v}}{\partial t} = \begin{cases} \rho_w^{-1}\operatorname{div}\boldsymbol{\sigma}_w & \text{in } \Omega_w, \\ \rho_b^{-1}\operatorname{div}\boldsymbol{\sigma}_b - (\mathbf{v}\cdot\nabla)\mathbf{v} & \text{in } \Omega_b. \end{cases} \tag{3.1}$$

For incompressible blood, the mass conservation equation reads:

$$\operatorname{div}\mathbf{v} = 0 \quad \text{in } \Omega_b. \tag{3.2}$$

On the interface between the blood and the wall, we assume the balance of normal stresses

$$\boldsymbol{\sigma}_b\mathbf{n} = \boldsymbol{\sigma}_w\mathbf{n} \quad \text{on } \Gamma_{bw}, \tag{3.3}$$

where $\mathbf{n}$ is the unit normal vector on Γ_{bw}. On the flow inlet one imposes the Dirichlet boundary condition $(u(\xi,t))$, whereas on the flow outlet the normal stress is balanced by the exterior pressure from the Windkessel model. On all boundaries of the vessel wall, except Γ_{bw}, one imposes the free-stress condition. Initial conditions are not important for us since we are focused on quasi-periodic flows caused by the inflow velocity (2.1).

The blood is considered to be Newtonian fluid:

$$\boldsymbol{\sigma}_b = -p\mathbf{I} + \mu_b(\nabla\mathbf{v} + \nabla\mathbf{v}^T) \quad \text{in } \Omega_b. \tag{3.4}$$

The wall is assumed to be a linear incompressible material with Lame constant μ_w: is

$$\boldsymbol{\sigma}_w = 2\mu_w\mathbf{E} - p_w\mathbf{I}, \qquad \mathbf{E} \coloneqq \frac{1}{2}\left(\nabla\mathbf{u} + \nabla\mathbf{u}^T\right), \tag{3.5}$$

where $\mathbf{u}$ is the displacement. The reference state ($\mathbf{u} = \mathbf{0}$) corresponds to the diastole.

The 3D FSI problem consists in finding pressure p, velocity $\mathbf{v}$ in Ω and displacement $\mathbf{u}$ in Ω_w satisfying the set of equations (3.1)–(3.5). The reference numerical solution of (3.1)–(3.5) denoted as *3dFSI* is based on a stabilized semi-discrete P1–P1 finite element (FE) method using an 'enhanced' membrane formulation [1]. Our goal is to compare various reduced models with the reference solution [1].

3.2. Reduced 1D model

The simplest reduced model is the 1D model of the bifurcation. Although it provides good agreement [1] with the numerical solution of (3.1)–(3.5), it does not provide the 3D flow in the bifurcation. However, the 1D model is an important component of multiscale models and has to be presented. The aortic bifurcation can be considered as three compliant vessels with a junction point. Assume that the ratio of each vessel diameter

to its length is relatively small. The reduced 1D model is based on the mass and momentum conservation laws which form a system of hyperbolic equations:

$$\partial A/\partial t + \partial(AU)/\partial x = 0, \tag{3.6}$$

$$\partial U/\partial t + \partial\left(U^2/2 + p/\rho_b\right)/\partial x = f_U, \tag{3.7}$$

where x is the coordinate along the vessel, $A(t,x)$ is the cross-section area of the vessel, $U(t,x)$ and p are the averaged over the cross-section linear velocity and blood pressure, ρ_b is the blood density, $f_U = -2(n+2)\mu_b \pi U A^{-1}\rho_b^{-1}$ is the flow acceleration due to friction derived under assumption of the axisymmetric velocity profile (2.1) [1].

In the 1D blood flow models, the conventional description of elastic properties of the vessel wall is provided by the pressure to cross-section area relationship $p(A)$ [1,3]:

$$P = P_d + \beta A_d^{-1}(\sqrt{A} - \sqrt{A_d}), \qquad \beta = 4\sqrt{\pi}Eh/3, \tag{3.8}$$

where A_d is the diastolic cross-sectional area, $P_d = 9.5$ kPa is the diastolic pressure. For a detailed discussion of the relationship we refer to [4,5].

The 1D flow equations in each vessel are coupled at the junction point by boundary conditions. The aortic bifurcation features a subsonic flow regime, therefore, for every vessel end point there exists one incoming and one outgoing characteristic of hyperbolic equations (3.6)–(3.7) which imposes a compatibility condition [6]. At the junction of N vessels one imposes conservation of mass and Bernoulli integral [7–9]

$$\sum_{k=k_1,k_2,\ldots,k_N} \varepsilon_k A_k U_k = 0, \qquad \frac{U_k^2}{2} + \frac{p_k(A_k)}{\rho_b} = P^l,\ k = k_1, k_2, \ldots, k_N, \tag{3.9}$$

where $\{k_1,\ldots,k_N\}$ are the indices of the incident vessels, $\varepsilon_k = 1$ (-1) for incoming (outgoing) vessels, p_k and P^l are the pressure and the total pressure at the junction point with index l, respectively. In total, at each junction one imposes $2N+1$ boundary conditions in terms of nonlinear algebraic equations. The boundary conditions are: the flow is prescribed on the inlet, the Windkessel model (2.2) is coupled to the outlets.

The numerical solution of (3.6)–(3.9) denoted as *1dHem* is based on the grid-characteristic method [10–12].

4. Multiscale models

Both conventional (3D FSI and 1D hemodynamics) models have practical deficiencies when one is interested in analyzing the 3D flow at the bifurcation: the full model is very complex and computationally expensive, the reduced model cannot reproduce the 3D flow. The remedy is provided by multiscale approaches.

4.1. 3D Navier–Stokes equations and their reduction

The rigid wall assumption reduces the system (3.1)–(3.5) to the conventional Navier–Stokes equations (3.1), (3.2), (3.4) in Ω_b. Velocity profile (2.1) defines the Dirichlet boundary condition at the inlet. At the outlet, we impose the Neumann boundary condition $\boldsymbol{\sigma}\mathbf{n} = p_1\mathbf{n}$, where $p_1(t)$ is the outlet pressure for the *1dHem* solution. The numerical solution of (3.1), (3.2), (3.4) denoted as *3dNS* is based on the Taylor–Hood FEM (P_2 for velocity, P_1 for pressure) for a quasiuniform tetrahedral mesh with 23532 cells with average size $h = 0.3$ cm. The method is implemented on the basis of the package Ani3D [13].

Eqs. (3.1), (3.2), (3.4) imply the solution of a 3D FE problem in the entire blood domain Ω_b which is still costly both for computer memory and computing time. Further reduction is based on the method of

asymptotic partial decomposition of the domain which is a combination of the 3D FE solution of (3.1), (3.2), (3.4) in a junction neighborhood Ω_j and analytical solutions to 1D problems in the cylindrical subdomains Ω'_a, $\Omega'_{i,1}$, $\Omega'_{i,2}$ [14]. The corresponding solution is denoted by *3dNSred*. The lengths of the abdominal and iliac branches in Ω_j are equal to $4r_a$ and $4r_i$, respectively. The lengths of the remaining 1D parts are: $l_{\Omega'_a} = 5.16$ cm, $l_{\Omega'_{i,1}} = l_{\Omega'_{i,2}} = 6.1$ cm. The number of cells in a quasiuniform tetrahedral mesh in Ω_j is 8304, therefore, the solution *3dNSred* is obtained at least 3 times faster than the solution *3dNS*. At each time step $t = k\Delta t$ one solves the 3D Navier–Stokes equations in Ω_j with Dirichlet boundary conditions and shifts the resulted 3D pressure field by $p_1(t) - p_{ext}(t)$ where p_{ext} is the pressure linearly extrapolated from Ω_j-outlets to the outlets of cylinders $\Omega'_{i,k}$. One sets the velocity on the inlet or outlet of Ω_j as the trace of a 3D velocity field $\mathbf{v}$ at the middle cross-section of Ω'_a or $\Omega'_{i,k}$ [15]. The field $\mathbf{v}$ is obtained by the "off line" solution of (3.1), (3.2), (3.4) in Ω'_a or $\Omega'_{i,k}$ with any profile on the boundary providing given fluxes. The flow rate $Q(t)$ defines the fluxes on inlet and outlet of Ω'_a, whereas $Q(t)$ and the ratio of fluxes at outlets of the iliac arteries for the solution *1dHem* with very stiff vessel walls define the fluxes in $\Omega'_{i,k}$. Impact of the profile on the boundary on the profile at the middle cross-section decays exponentially with $l_{\Omega'_{i,k}}$, $l_{\Omega'_a}$ [14]. It is shown [14] that the solution *3dNSred* approximates the solution *3dNS* in Ω_j with the accuracy $O(\varepsilon^M)$ in the $H^1(\Omega_j)$-norm, if $\mathrm{diam}(\Omega_j) \sim M\varepsilon|ln(\varepsilon)|$, where $\varepsilon = \max\{2r_a l^{-1}_{\Omega'_a}, 2r_i l^{-1}_{\Omega'_{i,1}}\}$, M is a positive integer.

4.2. 3D–1D two-scale model

In the vicinity of the junction Ω_j we consider the 3D Navier–Stokes equations (3.1), (3.2), (3.4) whereas the flow in the remaining part of Ω_b is described by the 1D hemodynamic equations (3.6)–(3.7). Continuity of the fluid flux and the normal stress is prescribed on the interfaces between 1D and 3D models. An iterative numerical algorithm matching 1D and 3D solutions is described in [16]. The Dirichlet boundary condition on the inlet of Ω_j and the Neumann boundary condition on the outlets of Ω_j are provided by the 1D solution on each matching iteration. The resulted numerical solution is denoted by *131d*.

4.3. 3D–1D–0D three-scale model

The three-scale model is derived from the two-scale model by insertion of 0D models between the 1D and 3D models. The 0D model represents an elastic sphere filled with blood and is formalized by a system of ODEs. The elastic spheres compensate the lack of compliance in the 3D domain with rigid walls. An iterative numerical algorithm for matching 0D, 1D and 3D solutions is described in [16]. The numerical solution is denoted by *10301d*.

5. Results and discussion

The numerical solutions *1dHem*, *3dNS*, *3dNSred*, *131d*, *10301d* are compared with the reference solution *3dFSI*. Fig. 5.1 demonstrates flow rate and pressure waveforms computed by different methods as well as their deviations from the reference *3dFSI* waveform. The waveforms of the solutions *1dHem*, *10301d* provide the best match to the reference waveform *3dFSI*.

Table 5.1 presents the average relative error *avg*%, the maximum relative error *max*%, the normalized errors for systolic and diastolic flux and pressure *sys*% and *dias*% defined in [1]. The three-scale solution *10301d* provides the minimal error for flux and pressure among the considered multiscale solutions providing the 3D flow in bifurcation neighborhood Ω_j. We explain the success of the three-scale model by incorporation of the 0D elastic spheres which add compliance to the model with rigid wall in the bifurcation. The two-scale models do not account compliance of the bifurcation region.

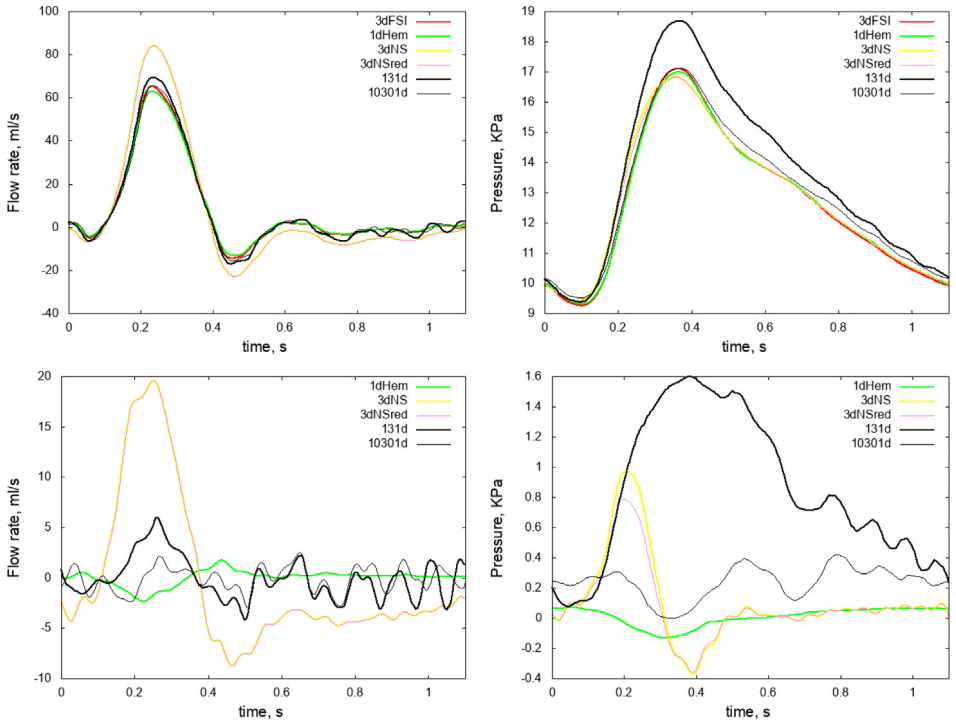

Fig. 5.1. Top row: Flow rate waveform (left) and pressure waveform (right) at the junction computed by different methods. Bottom row: deviations of these waveforms from the reference *3dFSI* waveform.

Table 5.1
Error at the junction in flow rate (left) and pressure (right) computed by different methods.

Error in method	Flux				Pressure			
	avg%	max%	sys%	dias%	avg%	max%	sys%	dias%
1dHem	0.78	3.53	−3.50	1.76	0.41	0.74	−0.63	0.32
3dNS	9.15	30.02	28.62	−13.13	1.41	8.31	−1.59	0.81
3dNSred	9.15	30.02	28.62	−13.13	1.40	8.26	−1.58	0.81
131d	2.51	9.13	6.12	−4.17	6.24	10.25	9.27	0.71
10301d	1.15	4.49	0.61	−1.79	2.02	3.48	0.13	1.59

Acknowledgments

We are thankful to Sergey Simakov and Timur Gamilov for helpful discussions and the 1D hemodynamic model. We also thank Alexander Danilov for generation of the computational meshes.

References

[1] N. Xiao, J. Alastruey-Arimon, C.A. Figueroa, A systematic comparison between 1D and 3D hemodynamics in compliant arterial models, Int. J. Numer. Methods Biomed. Eng. 30 (2) (2014) 204–231.

[2] C.G. Caro, T.J. Pedley, R.C. Schroter, W.A. Seed, The Mechanics of the Circulation, second ed., Cambridge University Press, 2012.

[3] E. Boileau, P. Nithiarasu, P.J. Blanco, et al., A benchmark study of numerical schemes for one-dimensional arterial blood flow modelling, Int. J. Numer. Methods Biomed. Eng. 31 (10) (2015) http://dx.doi.org/10.1002/cnm.2732.

[4] N. Bessonov, A. Sequeira, S. Simakov, Yu. Vassilevski, V. Volpert, Methods of blood flow modelling, Math. Model. Nat. Phenom. 11 (1) (2016) 1–25.

[5] Yu. Vassilevski, V. Salamatova, S. Simakov, On the elastisity of blood vessels in one-dimensional problems of hemodynamics, J. Comput. Math. Math. Phys. 55 (9) (2015) 1567–1578.

[6] Yu. Vassilevski, T. Gamilov, P. Kopylov, in: M. Papadrakakis, et al. (Eds.), Pesonalized Computation of Fractional Flow Reserve in Case of Two Consecutive Stenoses Proceedings of the VII European Congress on Computational Methods in Applied Sciences and Engineering, ECCOMAS Congress 2016, Crete, Greece, 5–10 June, Vol. 1, 2016, pp. 90–97.
[7] M.S. Olufsen, C.S. Peskin, W.Y. Kim, E.M. Pedersen, A. Nadim, J. Larsen, Numerical simulation and experimental validation of blood flow in arteries with structured-tree outflow conditions, Ann. Biomed. Eng. 28 (2000) 1281–1299.
[8] S. Sherwin, V. Franke, J. Peiró, K. Parker, One-dimensional modelling of a vascular network in space–time variables, J. Eng. Math. 47 (2003) 217–250.
[9] E. Ozawa, K. Bottom, X. Xiao R.D. Kamm, Numerical simulation of enhanced external counterpulsation, Ann. Biomed. Eng. 29 (2001) 284–297.
[10] A.S. Kholodov, Some Dynamical Models of External Breathing and Haemodynamics Accounting for their Coupling and Substance Transport, in: Computer Models and Medicine Progress, M.:Nauka, 2001, pp. 127–163, (in Russian).
[11] S.S. Simakov, A.S. Kholodov, Computational study of oxygen concentration in human blood under low frequency disturbances, Math. Models Comput. Simul. 1 (2009) 283–295.
[12] Yu. Vassilevskii, S. Simakov, V. Salamatova, Yu. Ivanov, T. Dobroserdova, Numerical issues of modelling blood flow in networks of vessels with pathologies, Russ. J. Numer. Anal. Math. Model. 26 (6) (2011) 605–622.
[13] K. Lipnikov, Yu. Vassilevski, A. Danilov, et al., Advanced Numerical Instruments 3D. http://sourceforge.net/projects/ani3d.
[14] G. Panasenko, K. Pileckas, Asymptotic analysis of the non-steady Navier–Stokes equations in a tube structure. I. The case without boundary layer-in-time, Nonlinear Anal. Ser A Theory Methods Appl. 122 (2015) 125–168.
[15] A. Nachit, G. Panasenko, A.M. Zine, Asymptotic partial domain decomposition in thin tube structures: numerical experiments, Int. J. Multiscale Comput. Eng. 11 (5) (2013) 407–441.
[16] T. Dobroserdova, M. Olshanskii, S. Simakov, Multiscale coupling of compliant and rigid walls blood flow models, Int. J. Numer. Methods Fluids 82 (12) (2016) 799–817.